

Floods and Adaptation Strategies: Evidence from Indian Manufacturing*

Marko Irisarri[†] Alejandro Rábano[‡] José Nicolás Rosas[§]

(Preliminary and Incomplete)

May 28, 2025

Abstract

We study how manufacturing establishments in India adapt to flood risk. Combining establishment-level data with geo-coded flood records and regional economic indicators, we examine how production and investment decisions respond to flood events conditional on historical exposure. We find that investment is more resilient in high-risk areas, consistent with forward-looking adaptation. To rationalize these findings, we propose a firm dynamics model featuring flood risk and private insurance to floods through a *flood preventing capital*. To overcome the course of dimensionality in this dynamic spatial model with aggregate uncertainty, we resort to Deep Learning techniques. We employ the model to quantify the aggregate economic impact of floods and evaluate the effectiveness of adaptation in mitigating climate-induced damages, and find that the proposed mechanism can replicate the patterns in the data.

Keywords:

JEL Classifications: O14, O53, Q54, R11, D25

*We thank our advisors Isaac Baley, Andrea Caggese, Davide Debortoli, Jordi Galí, David Nagy and Edouard Schaal for their constant guidance and support with this project. We are also grateful to Paula Bustos, Humberto Llavador and Jaume Ventura for insightful discussions that helped improving our paper, as well as participants in the CREi International Lunch, the BSE Jamboree 2023, the PSE 2023 Summer School on Climate Change and the SAEe 2023. This paper was previously circulated under the title “*The Transmission of Climate Shocks: The Case of Floods in India*”.

[†]Universitat Pompeu Fabra. Email: marko.irisarri@upf.edu. Web: <https://markoirisarri.github.io/>

[‡]Universitat Pompeu Fabra. Email: alejandro.rabano@upf.edu

[§]Universitat Pompeu Fabra. Email: josenicolas.rosas@upf.edu. Web: sites.google.com/view/jnrosas

1 Introduction

As global temperatures rise beyond 1°C above pre-industrial levels, the severity and frequency of extreme weather events are expected to increase.¹ Historically, some regions have been more frequently exposed to such events, prompting firms operating in those areas to adapt their economic activities to the recurring threat of natural disasters. While a growing literature has examined the role of plant location and supply chain reorganization as adaptation strategies, we still know relatively little about how firms undertake private investments in adaptation aimed at mitigating the economic impact of extreme weather events. A more detailed understanding of such investments is essential for anticipating where climate-related damages will be most severe and for designing effective policy responses that reduce the long-run costs of climate change.

Among the various extreme weather events, floods are particularly damaging. In India alone, they result in the loss of approximately 1,600 lives annually and cause economic damages equivalent to 0.2% of GDP each year ([National Disaster Management Authority, Government of India, 2023](#)). Floods occur recurrently during the monsoon season; while their exact timing and location are difficult to predict, some regions have historically been more exposed than others. This setting provides a natural context to study adaptation: firms operating in flood-prone areas can anticipate the likelihood of recurrent floods and make forward-looking investments to mitigate their impact. If firms adapt based on local flood recurrence, then we should expect a given flood to have a larger economic impact in locations where floods are historically rare and, correspondingly, where adaptation is limited.

In the first part of the paper, we study the dynamic causal effects of *extreme* and *severe* floods on Indian manufacturing production and investment by constructing a panel of establishments from the Annual Survey of Industries (ASI) for the period 2000–2007. The ASI provides detailed balance sheet data and district-level identifiers, which we merge with geocoded flood records from the Dartmouth Flood Observatory (DFO). Floods in this setting arise from various meteorological and hydrological phenomena and are likely exacerbated by climate change. These events can disrupt production through multiple channels, including direct damage to facilities, impediments to the movement of goods and labor, and broader supply chain disruptions. Crucially, the timing and location of flood events are plausibly exogenous to local industrial dynamics, allowing for credible identification. In addition, the availability of historical flood data prior to our sample period enables us to assess whether the economic impact of floods varies with long-run exposure, providing insight into firms' adaptive responses to climate risk.

Using an event-study design, we document that the impact of floods on manufacturing establishments depends crucially on a district's historical exposure to such events. In districts with low pre-2000 flood exposure, we find that severe or extreme floods lead to persistent

¹See the IPCC Sixth Assessment Report ([Pörtner et al., 2022](#)).

declines in both output and capital accumulation, with effects that grow over time. In contrast, establishments located in historically flood-prone districts experience no significant output losses and, if anything, respond with increased investment in capital following a flood event. These findings suggest that firms operating in high-exposure regions may have adapted more effectively to climate risk—either through physical resilience, supply chain adjustments, or precautionary investment—thereby dampening the adverse economic consequences of future floods.

To rationalize these findings, we propose a firm dynamics dynamic spatial model à la [Khan and Thomas \(2008\)](#). In the model economy, there exist multiple locations with heterogeneous exposure to flood risk, with some regions being more likely to experience a flood than others. Upon a flood, firms in the affected locations experience a destruction of their stock of production capital and production. To privately insure against these extreme climate events, firms are able to invest in a *flood preventing capital*. Investing in this capital allows the firms to mitigate the damages caused by flooding.

We take this model to an economy with two regions, where the flood probabilities are estimated from the data and the firm side employs a standard firm-dynamics calibration. We find that firms in the Risky Region invest more in the flood preventing capital than their counterparts in the Safer Region. This necessity to invest more heavily in flood preventing capital in the Risky Region drains the resources of firms at the risky-steady state, and their discounted sum of profits is lower than in the Safer Region. However, this investment in the adaptation mechanism provides a key benefit. When employing the model as a laboratory to study the responses of both economies to a flood shock, we find that all the aggregates of interest (including capital and production) experience larger declines in the Safer Region. Thus, the proposed flood preventing accumulation mechanism is able to rationalize the findings in the data.

Related Literature

First, this paper contributes to a growing literature on the effects of floods on output and investment. In the context of coastal flooding, [Desmet et al. \(2021\)](#) incorporate sea level rise projections into a dynamic spatial model with endogenous investment and migration, while [Balboni \(2025\)](#) studies the role of infrastructure networks in shaping the impact of flooding in Vietnam. For the United States, [Jia et al. \(2025\)](#) analyze the macroeconomic implications of changing flood risk, and [Pang and Sun \(2024\)](#) examine how post-hurricane relief policies influence mobility decisions. In India, [Pelli et al. \(2023\)](#) document reallocation of output and capital toward better-performing industries following cyclones, [Rao et al. \(2022\)](#) highlight sectoral heterogeneity in the effects of excess rainfall, and [Hossain \(2020\)](#) shows that labor reallocates toward the informal sector after floods. We contribute to this literature by documenting that the economic impact of severe floods on manufacturing establishments in India is significantly larger in districts with low historical exposure. Our identification strategy leverages the difference-in-differences estimator proposed by

[De Chaisemartin and d'Haultfoeuille \(2024\)](#), which accounts for heterogeneous and dynamic treatment effects. Relatedly, [Gandhi et al. \(2022\)](#) find that cities with greater historical flood exposure are less affected by current events, consistent with our interpretation of adaptation in the manufacturing sector.

Second, this paper also contributes to a recent set of studies on firm-level adaptation to climate change. A number of recent papers emphasize the role of supply chain reorganization: [Pankratz and Schiller \(2024\)](#) show that customers terminate trade relationships when suppliers are hit by extreme weather events, [Castro-Vincenzi et al. \(2024\)](#) find that firms diversify input purchases in response to flood risk, and [Balboni et al. \(2024\)](#) document that firms adjust to climate disruptions by choosing safer transport routes. Multinational firms in [Castro-Vincenzi \(2024\)](#) adapt by selecting plant locations and capacities to hedge against flood-related disruptions, while [Albert et al. \(2024\)](#) examine how labor and capital reallocate in response to drought in Brazil. Public investment by local authorities in flood defence mitigates the impact of floods in [Ficarra and Mari \(2025\)](#). In the Indian manufacturing context, [Somanathan et al. \(2021\)](#) show that air-conditioning mitigates productivity losses from extreme temperatures. Another adaptation channel is given by the investment into specific forms of capital that reduce the vulnerability to floods. [Fried \(2022\)](#) considers this type of investment in the US, focusing on idiosyncratic flood shocks. Compared to her work, we introduce aggregate uncertainty and document empirically the heterogeneous impact of floods depending on previous exposure in an emerging economy.

Lastly, this paper is related to the emerging literature advocating for the use of Deep Learning in order to solve complex DSGE models with aggregate uncertainty and rich individual heterogeneity. Solving this class of models is computationally infeasible due to the curse of dimensionality when employing traditional methods such as [Krusell and Smith \(1998\)](#). Several papers have provided methodological contributions, including [Maliar et al. \(2021\)](#), [Han et al. \(2021\)](#), [Kahou et al. \(2021\)](#) and [Azinovic et al. \(2022\)](#). The main idea of these methods is to construct Neural Network approximators for the policy and value functions of interest, thus avoiding the curse of dimensionality as Neural Networks are trained by sampling data, which scales linearly in the number of dimensions. There already exists a literature implementing these methods in the context of climate-related DSGE models such as [Pang and Sun \(2024\)](#), who study the welfare impact of U.S. disaster relief policies. In this paper, we employ these methodologies in a dynamic spatial model with aggregate flood uncertainty and provide an implementation of [Han et al. \(2021\)](#) with multiple controls and auxiliary Neural Network approximators for equilibrium prices.

The remainder of the paper is structured as follows. First, section 2 presents the data and the obtained empirical results. Secondly, section 3 discusses the proposed model. Third, section 4 shows the employed calibration and solution methodology. Fourth, section 5 presents the results of the model, including the risky steady-state investment in each type of capital by region and the obtained IRFs to a flood shock. Lastly, section 6 concludes.

2 Empirical Evidence

In this section, we estimate the effect of extreme and severe floods on Indian manufacturing production and investment using detailed plant-level data between 2000-2019 and data on historical floods since 1985.

2.1 Data

2.1.1 Panel of Manufacturing Establishments

To analyze the impact of floods on firm-level outcomes, we use data from the Annual Survey of Industries (ASI), the most comprehensive panel available for registered manufacturing establishments in India. The ASI, administered by the Government of India, covers all large factories (those employing more than 100 workers) and a rotating random sample of roughly one-fifth of smaller registered plants under the Indian Factories Act. Large establishments are surveyed annually, while smaller ones appear in the sample on a staggered basis. The unit of observation is the establishment (referred to as a “factory” in ASI documentation).

While the ASI cross-sectional files contain district identifiers, these are absent from the panel dataset. To address this, we follow the approach of [Martin et al. \(2017\)](#), merging the cross-sectional and panel datasets to recover district-level identifiers. Our analysis uses data from 2000–01 to 2007–08, the period for which this matching is feasible. The ASI provides rich annual data on key establishment-level variables, including total output, fixed assets, debt, cash holdings, inventories, input expenditures, and employment, disaggregated by production and non-production workers.

Our primary variables of interest will be total output and capital. Total output is defined as the ex-factory value² of products and by-products manufactured, in addition to a range of other receipts. Capital is measured as the depreciated value of fixed assets—land, buildings, plant, and machinery—owned by the establishment on the final day of the accounting year.

Over time, the Government of India has reorganized administrative boundaries and updated industry classifications. Specifically, district boundaries have been split into smaller units, and the industrial classification system has transitioned from NIC-1998 to NIC-2004 and NIC-2008. To ensure consistency in geographic and industry identifiers across years, we adopt the concordance tables developed by [Martin et al. \(2017\)](#). Using these mappings, we construct a balanced panel of 478 constant-boundary districts, each of which has at least one manufacturing establishment observed during our study period.

²The ex-factory value includes the net sale value (inclusive of subsidies) of all products and by-products manufactured, as well as other receipts such as income from non-industrial services rendered, contract work using externally supplied materials, the value of electricity produced and sold, sale value of resold goods, additions to inventories of semi-finished goods, and own-account construction.

2.1.2 Flood Events

We obtain data on historical flood events from the *Global Active Archive of Large Flood Events* maintained by the Dartmouth Flood Observatory (DFO). The DFO compiles this archive using a range of sources, including news reports, government bulletins, satellite imagery, and remote sensing technologies. Each entry is associated with an “affected area” map that delineates the geographic extent of a discrete flood event.

We use these map outlines to perform a geospatial join, assigning each flood event to one or more districts in India. For each event, the DFO records the estimated start and end dates, the underlying causes, the geographic footprint, and several indicators of severity and damage. The archive begins in 1985 and is continuously updated.

In our analysis, we focus on the most economically consequential floods. Specifically, we use the DFO’s severity scale, which ranges from 1.0 to 2.0 in increments of 0.5, and concentrate on events classified as either **severe** or **extreme**. These categories are defined as follows:

1. Severe floods (Severity = 1.5):

- Estimated worldwide recurrence interval between 20 and 100 years, *and/or*
- Local recurrence interval of 10–20 years with a large geographic footprint ($>5,000 \text{ km}^2$)

2. Extreme floods (Severity = 2.0):

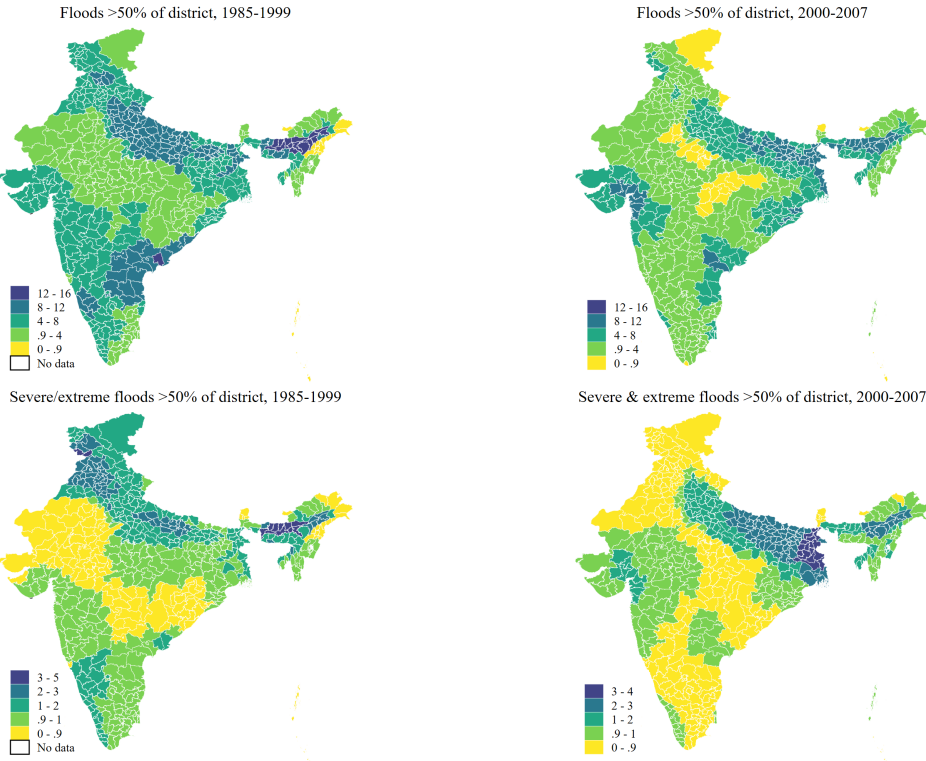
- Estimated worldwide recurrence interval exceeding 100 years

Building on the DFO flood severity classification, we construct extensive and intensive margin measures to quantify flood exposure at the district level. For the *extensive* margin, we define a set of binary indicators equal to one if at least one *severe* or *extreme* flood (severity ≥ 1.5) in a given year affects more than 50%³ of a district’s area, and zero otherwise. These indicators are assigned uniformly to all establishments within the affected district, based on their geographic location. For the *intensive* margin, we construct count variables capturing the number of *severe* or *extreme* floods in a given year that cover more than 50% (or 100%) of the district area. Applying these definitions, we identify 15 district-level severe/extreme flood events in India between 2000 and 2007.

Figure 1 presents the geographic distribution of flood exposure across Indian districts, both during our sample period and over a longer historical horizon. The top panels display exposure to all recorded flood events, while the bottom panels focus on *severe* and *extreme*

³As a robustness check, we re-estimate our main specifications using an alternative definition of flood exposure, where the binary indicators equal one only if a flood covers 100% of a district’s area in a given year. The main qualitative results remain robust to this stricter definition.

Figure 1: Exposure to floods in Indian districts across time



Notes: District-level flood exposure based on events that affected more than 50% of a district's area. The top panels display exposure to all recorded flood events, while the bottom panels focus on *severe* and *extreme* floods, as defined in the main text. The left column corresponds to the period 1985–1999, and the right column to the period 2000–2007. *Source:* ML Infomap, the Dartmouth Flood Observatory and authors' own calculations.

floods, as defined earlier. During the 2000–2007 period, the northeastern and western regions experienced the highest frequency of high-severity floods. Historically, significant flood activity is also observed in the northern and southern regions. We exploit this spatial variation in flood exposure as part of our event study identification strategy.

2.1.3 Descriptive Statistics

Table 1 reports the mean and standard deviation of our main establishment-level variables: total output (y) and capital stock (k), along with some other relevant measures of labor input (l), labor productivity (lp) and wages (w). Summary statistics cover the period 2000–2007 and are shown separately for establishments located in districts that experienced at least one *severe* or *extreme* flood (as defined by our extensive margin measure) and those in unaffected districts. Column (1) presents the mean and standard deviation for firms in flood-affected districts, while Column (2) reports the same for unaffected areas. Column (3) shows the difference in means between the two groups, along with the corresponding t -statistic from a mean comparison test.

Only 13.34% of establishments in our sample are located in districts affected by at least one *severe* or *extreme* flood during our period of analysis. Firms in flood-affected districts

Table 1: Summary statistics: Firms in districts affected or not by severe/extreme floods

	(1)		(2)		(3)	
	S/E Flood	No S/E Flood			Diff.	
	Mean	SD	Mean	SD	b	t
y	16.99	2.29	16.91	2.23	-0.08***	(-5.86)
k	15.28	2.63	15.29	2.61	0.01	(0.41)
l	3.95	1.49	3.98	1.46	0.03**	(3.15)
lp	13.04	1.48	12.93	1.47	-0.11***	(-12.20)
w	10.54	0.85	10.53	0.82	-0.00	(-0.45)
Observations	31,119		202,001		233,120	

display statistically significantly higher average total output (y) and labor productivity (lp), with magnitudes of 0.08 and 0.11 log points, respectively, both significant at the 1% level. Average employment (l) is modestly but significantly lower—by 0.03 log points—at the 5% level. In contrast, we find no statistically significant differences in average capital stock (k) or wages (w) across the two groups.

Standard deviations for all five variables are consistently higher among establishments in flood-affected districts, suggesting greater within-group heterogeneity. This may reflect differential exposure, variation in adaptation capacity, or nonlinear effects of flood events across firms within the same region.

2.2 Econometric Methodology

Our identification strategy exploits variation in the timing and intensity of exposure to *severe* and *extreme* floods across districts and over time. A popular method to estimate the causal effect of these types of “treatments” on an outcome is to compare over time groups experiencing different evolutions of their exposure to treatment, which is commonly referred to as the generalized differences-in-differences approach. This approach compares changes in outcomes across groups (*districts*) that experience differential exposure to treatment at different points in time.

In practice, this idea is implemented by estimating specifications of the form:

$$Y_{g,t} = \alpha_g + \lambda_t + \beta D_{g,t} + \varepsilon_{g,t},$$

where Y_{gt} denotes the outcome of interest for group g in period t , α_g are group (district) fixed effects, λ_t are time fixed effects, and D_{gt} is a treatment indicator capturing exposure to a *severe* or *extreme* flood. The coefficient β identifies the average effect of flood exposure, under the assumption of parallel trends.

Such two-way fixed effects (TWFE) regressions are among the most widely used methods in empirical economics for estimating the effect of a treatment on an outcome. Motivated by the fact that, in a simple two-period, two-group setup, the difference-in-differences (DiD)

estimator corresponds to the treatment coefficient from a TWFE regression, researchers have commonly applied TWFE specifications in more complex settings involving multiple groups and periods, staggered treatment adoption, treatment reversals, or non-binary treatments.

However, recent work has shown that in such extended designs, the TWFE estimator identifies a causal average treatment effect (ATE) only under a set of stringent assumptions: (i) the parallel trends assumption must hold; (ii) there are no anticipation effects; and (iii) the treatment effect is constant across groups and over time. While the first two assumptions are commonly discussed in applied work, the third—constant treatment effects—is often overlooked and unlikely to hold in many empirical settings. As emphasized by [de Chaisemartin and D'Haultfoeuille \(2023\)](#), violations of this assumption can lead to biased or misleading estimates, prompting a growing literature that diagnoses the issue and proposes alternative estimators.

In our setting, in addition to the standard identification assumptions of no anticipation, treatment exogeneity, and parallel trends, several features of the treatment process introduce further complications. Unlike the canonical difference-in-differences (DiD) setup, where treatment is binary and absorbing—i.e., once treated, a unit remains treated—our treatment is non-absorbing. Districts may experience a *severe* or *extreme* flood in one year but not in others, allowing for multiple entries into and exits from treatment over the sample period. This temporal variability violates assumptions underlying many conventional two-way fixed effects (TWFE) estimators.

Moreover, the effects of flood exposure may be heterogeneous across both time and cohorts. Establishments are affected by treatment at different points during the sample, and the average treatment effect may vary depending on whether a district is exposed earlier or later. Additionally, we cannot rule out dynamic treatment effects—where the impact of a flood persists, attenuates, or intensifies over time—further complicating causal interpretation. These issues motivate the use of alternative estimation strategies that can accommodate non-absorbing treatments and heterogeneous or dynamic effects.

To address the concerns outlined above, we follow [Castro-Vincenzi \(2024\)](#), who studies a similar setting, and implements the estimator proposed by [De Chaisemartin and d'Haultfoeuille \(2024\)](#). This is a difference-in-differences estimator designed to recover contemporaneous and dynamic treatment effects in settings with heterogeneous effects and non-absorbing treatment. The estimator generalizes the event-study framework by defining the “event” as the first time a group changes its treatment status. It then compares the evolution of outcomes in treated groups to that of untreated control groups with the same initial treatment status.

Formally, let F_g denote the first period in which group g experiences a change in treatment. The estimator of the expected difference between group g 's actual outcome at time F_g –

$1 + l$ and its counterfactual “status quo” outcome if its treatment had remained equal to its period-one value from period one to $F_g - 1 + l$ is given by:

$$\text{DID}_{g,\ell} = Y_{g,F_g-1+\ell} - Y_{g,F_g-1} - \frac{1}{N_{F_g-1+\ell}^g} \sum_{g': D_{g',1} = D_{g,1}, F_{g'} > F_g - 1 + \ell} (Y_{g',F_g-1+\ell} - Y_{g',F_g-1}) \quad (1)$$

where $Y_{g,F_g+\ell}$ corresponds to the outcome of interest for group g at moment $F_g - 1 + \ell$, or ℓ periods after group g received the treatment for the first time in period F_g , Y_{g,F_g-1} corresponds to the same outcome of interest for group g one period before it changes treatment status for the first time, and $N_t^g = \#\{g' : D_{g',1} = D_{g,1}, F_{g'} > t\}$ is the number of groups g' with the same period-one treatment as g , and that have kept the same treatment from period 1 to t ([De Chaisemartin and d'Haultfoeuille, 2024](#)).

Intuitively, this DID estimator compares the change in outcomes from period $F_g - 1$ to $F_g - 1 + \ell$ for group g —which experiences a treatment change at time F_g —to the average outcome change over the same period for groups that (i) share the same baseline treatment status ($D_{g',1} = D_{g,1}$) and (ii) have not experienced a treatment change by period $F_g - 1 + \ell$. This comparison isolates the effect of transitioning into treatment, controlling for underlying trends among comparable, untreated groups ([Castro-Vincenzi, 2024](#); [De Chaisemartin and d'Haultfoeuille, 2024](#)).

In addition, [De Chaisemartin and d'Haultfoeuille \(2024\)](#) define an estimator for the non-normalized event-study effects, which aggregates the group-specific $\text{DID}_{g,\ell}$ estimates across all eligible groups. This estimator is given by:

$$\text{DID}_\ell = \frac{1}{N_\ell} \sum_{g: F_g - 1 + \ell \leq T_g} S_g \cdot \text{DID}_{g,\ell} \quad (2)$$

where T_g denotes the last period for which there exists a group with the same period-one treatment status as group g and no treatment change since the beginning of the panel. The term $N_\ell = \#\{g : F_g - 1 + \ell \leq T_g\}$ is the number of groups for which $\text{DID}_{g,\ell}$ can be estimated at event time ℓ , and $S_g = 1\{D_{g,F_g} > D_{g,1}\} - 1\{D_{g,F_g} < D_{g,1}\}$ indicates the direction of treatment change: it equals 1 for groups whose treatment increases at F_g and -1 for those whose treatment decreases ([De Chaisemartin and d'Haultfoeuille, 2024](#)).

Intuitively, this estimator captures the average effect of being exposed to a weakly higher level of treatment for ℓ periods, by comparing changes in outcomes for groups whose treatment level changes relative to otherwise similar groups with unchanged treatment status.

To fix ideas, in our setting each group g corresponds to a district (or set of districts) that experiences a change in treatment status—defined as exposure to a *severe* or *extreme* flood—for

the first time in year F_g . Since treatment is assigned at the district level, but outcomes are observed at the establishment level, our setup involves a mismatch between the level of treatment and the level of outcome measurement.

The estimators proposed by [De Chaisemartin and d'Haultfoeuille \(2024\)](#) can accommodate such settings. Specifically, the `did_multiplegt_dyn` command that implements the estimators proposed in their work allows for data that is more disaggregated than the (g, t) level. When establishment-level data is provided, the command internally aggregates outcomes to the (g, t) level, and automatically weights each (g, t) cell by the number of underlying observations. This feature enables us to estimate group-time average treatment effects while preserving consistency with the group-level treatment variation.

2.3 The Impact of Extreme Flooding on Firm-level Outcomes

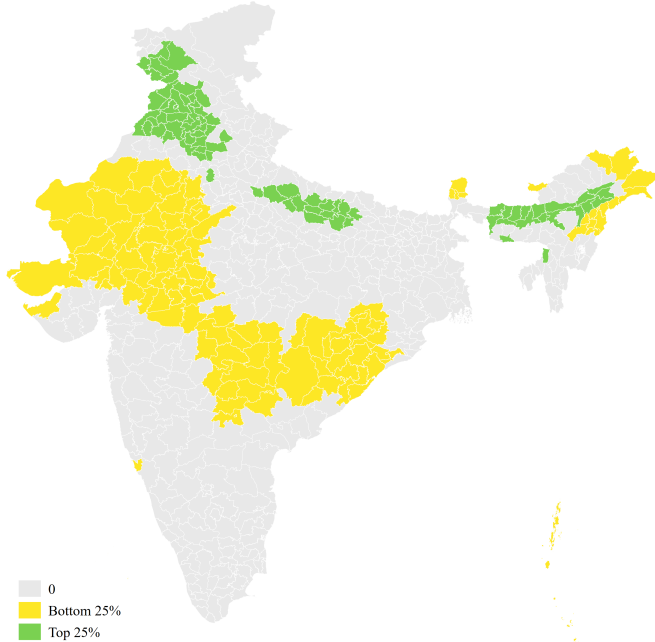
As noted in the previous section, Figure 1 illustrates a central feature of our empirical setting: the pronounced geographic variation in flood exposure across Indian districts. The bottom-left panel provides further context by documenting historical exposure to *severe* and *extreme* floods during the pre-sample period (1985–1999). Several districts in the northeast and north experienced recurrent high-severity floods, while much of central and western India saw little or no such activity. This variation reflects persistent climatic and geographic patterns that have also shaped historical exposure. Such spatial differences are central to our identification strategy and form the basis of our cross-sectional heterogeneity analysis, as they allow for comparisons between districts with systematically different flood risk profiles.

To explore this dimension more systematically, we classify districts into quartiles based on their cumulative exposure to *severe* and *extreme* floods between 1985 and 1999, as shown in Figure 2. We focus on the top 25% of historically exposed districts (shown in green) and the bottom 25% (shown in yellow). This grouping enables a test of whether the economic effects of flood events differ with long-run exposure—under the hypothesis that firms in historically flood-prone areas may have adapted more extensively to mitigate the impacts of recurrent climate risk.

We start by estimating the effect of a severe or extreme flood on establishment-level output and capital, comparing districts with high versus low historical exposure to such events. To ensure that the treatment and control groups are appropriately defined, we restrict the estimation sample to establishments that had not experienced a flood at baseline. Specifically, we exclude all firms located in districts that were treated in the first period of our sample (2000), as well as those exposed to floods in the two years immediately prior (1998–1999). This restriction guarantees that all included establishments share a common pre-treatment status and enables a clean interpretation of our estimates as the effect of transitioning from no exposure to exposure to a severe or extreme flood, relative to a counterfactual in which the district remained unexposed ([De Chaisemartin and d'Haultfoeuille, 2024](#)).

Figure 2: Historical exposure to floods in Indian districts: top and bottom quartiles

Severe & extreme floods >50% of district, 1985-1999

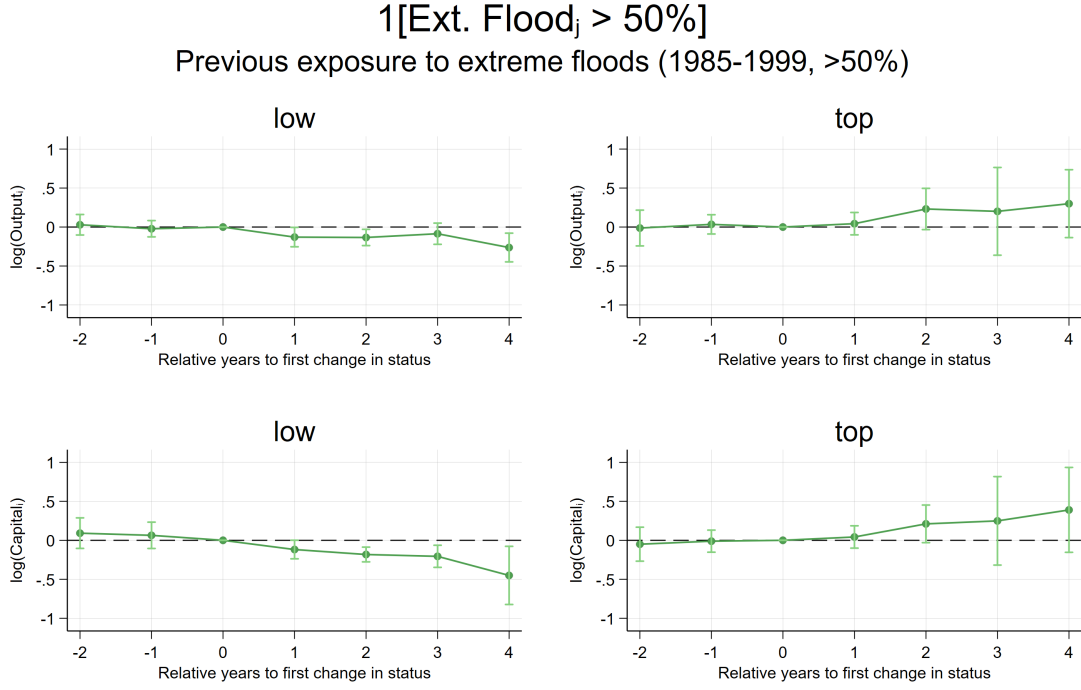


Notes: District-level historical flood exposure based on events that affected more than 50% of a district's area.
Source: ML Infomap, the Dartmouth Flood Observatory and authors' own calculations.

Figure 3 presents the non-normalized event-study estimates (Eq. 1) of the dynamic effects of severe or extreme floods on establishment-level outcomes, separately for districts with low and high historical exposure to flooding. The top panels show the trajectory of log output around the first incidence of a flood event covering more than 50% of a district's area up to 4 years after the first flooding event ($\ell = 4$). In low-exposure districts (left panel), output declines steadily after treatment, reaching a cumulative drop of approximately 0.5 log points by year four relative to production in plants in districts that have not been yet treated. Although confidence intervals are wide, the downward trend is persistent and suggests that floods impose lasting disruptions in regions with limited prior exposure. In contrast, the corresponding panel for high-exposure districts (right) reveals no meaningful post-flood decline in output. If anything, the trajectory slightly increases over time, though not significantly. These contrasting patterns suggest that prior exposure to floods may have induced forms of resilience or adaptation that mitigate the production losses associated with new flood shocks.

The bottom panels display a similar pattern for capital. In low-exposure districts, capital stock begins to decline immediately following the first flood event and continues to fall over the subsequent years, consistent with a disinvestment response or flood-related capital destruction. By contrast, in high-exposure districts, capital appears to increase modestly in the years following the shock. While the estimates are imprecise, the upward trajectory is suggestive of a potential adaptation margin—firms in historically exposed regions may

Figure 3: Effect of severe-extreme floods on establishment-level outcomes by degrees of historical exposure



Analytical standard errors are clustered at the district level. 90% confidence intervals relying on a normal approximation are displayed.

Notes: District-level historical flood exposure based on events that affected more than 50% of a district's area between 1985-1999. Non-normalized event study estimators of the dynamic effects of an extreme/severe flood are computed as in Eq. 1. Standard errors are clustered at the district level, and 90% confidence intervals relying on a normal approximation are displayed. District-specific linear trends are included in the estimation.

respond by reinforcing or upgrading physical capital to buffer against the recurrence of flood shocks. Taken together, the event-study plots support the hypothesis that historical exposure facilitates adaptive investment, thereby reducing the long-run economic impact of severe and extreme floods.

3 Model

We propose a dynamic spatial equilibrium model of firm dynamics that aims to rationalize the stylized facts documented in the previous section. Primarily, it allows to study how firms may adapt to aggregate flood risk on the intensive margin by accumulating flood preventing capital. The model borrows insights from the literature on dynamic models of economic geography ([Kleinman et al. \(2023\)](#); [Giannone et al. \(2020\)](#)) as well as the one on firm dynamics ([Khan and Thomas \(2008\)](#); [Winberry \(2021\)](#)).

3.1 Environment

3.1.1 Geography

We assume that there is a discrete number of locations N , indexed by $l \in \{1, 2, 3, \dots, L\}$. Locations differ in two key dimensions. First, each location has its own stochastic process for the flood risk Γ_l . Thus, some locations are riskier than others. A region may be either flooded or non-flooded $a_l \in \{\text{flood}, \text{no flood}\}$. Second, locations are heterogeneous with respect to the size of their population L_n , and the aggregate population in the economy is a unit continuum $\sum_{l=1}^L L_l = 1$.

3.1.2 Trade and Goods

For simplicity, we assume that there exists a single final good Y that is produced by firms in all locations and is costlessly tradable. Therefore, prices thereof equalize across space $p_l = p \forall n$.

3.1.3 Firms

The firm side builds heavily on [Khan and Thomas \(2008\)](#), with the addition of convex costs and the access to the flood preventing capital k^f .

Firms in this economy have access to two types of capital: a production capital k and a flood preventing capital k^f whose role is to mitigate the damages caused by floods. We assume that upon a flood realization in location l , \mathbb{I}_{a_l} , all firms in that location suffer a loss $1 - F(k_f)$ of both capital and production in that period ⁴. We assume that $F(k^f)$ is concave, bounded between 0 and 1, $0 < F(k^f) < 1$ and increasing. Since the focus is on the adaptation of firms on the intensive margin, no mobility is allowed.

Time is discrete and there exists a unit continuum of firms $j \in [0, 1]$. To ease notation, we define the retained fractions of capital and output as $R_{t,j} = \mathbb{I}_{\{a_{l,t}=0\}} + \mathbb{I}_{\{a_{l,t}=1\}}F(k_{j,t}^f)$. Where \mathbb{I}_{a_l} is the indicator of whether the location is flooded or not, $(F(k_{j,t}^f))$ is the fraction of both output and capital that the firm retains in the event of a flood. That is, firms keep the full stock of production and capital if there is no flood, and retain a fraction $F(k_{j,t}^f)$ in the event of a flood. They produce the final good according to the following production function:

$$y_{j,t} = R_{t,j} z_{j,t} \left((R_{t,j} k_{j,t})^\alpha n_{j,t}^{1-\alpha} \right)^\mu \quad (3)$$

Where $z_{j,t}$ is the idiosyncratic productivity of the firm, α is the share of capital in production, μ is the returns to scale parameter, $k_{j,t}^f$ is the stock of flood preventing capital of a firm, $k_{j,t}$ is the stock of production capital of a firm and $n_{j,t}$ is the hired labour.

⁴This is motivated by the fact that the flood may hit at any point during the period, potentially damaging both the stock of capital and the stock of inventories already produced.

The idiosyncratic shock is independent across firms and locations but follows an autocorrelated AR(1) process within firms:

$$\log z_{j,t+1} = \rho_z \log z_{j,t} + \epsilon_{t+1}, \text{ where } \epsilon \sim N(0, \sigma_z) \quad (4)$$

Firms in this economy observe the aggregate state of the economy, which includes the realization of flood shocks in each location $a_{t,l}$ and prices for labour $w_{t,l}$. Then, they produce the final good $y_{j,t}$ by employing their retained stock of capital $R_{t,j}$ and labour $l_{j,t}$, which they hire period-by-period on the local labour market.

After production takes place, firms decide how much they want to invest in both the production and flood preventing capitals. We assume that both capitals are subject to the same depreciation rate and that both stocks get damaged in the event of a flood. We denote investment in flood preventing capital by $i_{j,t}^f = k_{j,t+1}^f - (1-\delta)R_{t,j}k_{j,t}^f$ and investment in production capital by $i_{j,t} = k_{j,t+1} - (1-\delta)R_{t,j}k_{j,t}$. Lastly, upon (non-zero) investment, firms must pay convex adjustment costs $\phi(\frac{i_{j,t}}{k_{j,t}})^2 k_{j,t}$ and $\phi(\frac{i_{j,t}^f}{k_{j,t}^f})^2 k_{j,t}^f$ for production and flood preventing capital, respectively.

3.1.4 Households

There exists a homogeneous unit continuum of exogenously distributed households across locations that satisfies $\sum_{l=1}^L L_n = 1$.

The preferences thereof are represented by the following expected utility function:

$$\mathbf{E} \sum_{t=0}^{\infty} \log \left(C_{t,l} - \xi \frac{N_{t,l}^{1+\eta}}{1+\eta} \right) \quad (5)$$

Which corresponds to the expected discounted sum of GHH (Greenwood et al., 1988) flow period utilities⁵. $C_{t,l}$ denotes consumption at time t in location l and $N_{t,l}$ is the counterpart for the labour supply. ξ regulates the disutility from labour and η is the Frisch elasticity. We assume that households in this economy are immobile. In addition, they are assumed to be hand to mouth and consume their labour income period by period $C_{t,l} = W_{t,l}N_{t,l}$. Furthermore, we assume that firms are owned by risk-neutral foreign investors, so that the relevant discount factor for the firms is constant and equal to the reciprocal of the interest rate, $\beta = \frac{1}{1+r}$.

⁵These preferences have the convenient feature of eliminating the wealth effect from the labour supply and essentially collapsing the household side to a static problem.

3.2 Firm's Optimization

The firm's individual states include the location $l_{j,t}$, idiosyncratic productivity $z_{j,t}$, stock of production capital $k_{j,t}$ and flood preventing capital $k_{j,t}^f$. The aggregate state vector \mathbf{S}_t in term includes the state of flooding in each location $\{a_l\}_{l=1}^L$ as well as the entire distribution of firms over the state space, $\mu(l, z, k, k^f)$. Embedding the dynamics of the aggregate state \mathbf{S}_t is necessary in this setting due to the presence of aggregate uncertainty stemming from the aggregate flood risk by region.

Given this setting, the Bellman Equation for the firm can be written as:

$$\begin{aligned}
 V(l, z, k, k^f; \mathbf{S}) &= \max_{n, k', k'^f} \pi(l, z, k, k^f; \mathbf{S}) + \beta \mathbf{E} \left(V(l', z', k', k'^f; \mathbf{S}') \right) \\
 \pi(l, z, k, k^f; \mathbf{S}) &= \underbrace{R(\mathbf{S})z ((R(\mathbf{S})k)^\alpha n^{1-\alpha})^\mu}_{\text{Production}} - \underbrace{w(\mathbf{S})n}_{\text{Labour Costs}} \\
 &\quad - \underbrace{(k' - (1 - \delta)R(\mathbf{S})k)}_{\text{Investment Production Capital}} - \underbrace{(k'^f - (1 - \delta)R(\mathbf{S})k^f)}_{\text{Investment Flood Preventing Capital}} \\
 &\quad \underbrace{\frac{\phi}{2} \left(\frac{(k' - (1 - \delta)R(\mathbf{S})k)}{k} \right)^2 k - \frac{\phi}{2} \left(\frac{(k'^f - (1 - \delta)R(\mathbf{S})k^f)}{k^f} \right)^2 k^f}_{\text{Convex Costs}}
 \end{aligned} \tag{6}$$

Where $V(l, z, k, k^f; \mathbf{S})$ is the Value Function of the firm and the expectation operator \mathbf{E} is with respect to idiosyncratic shocks, aggregate flood shocks and future prices. Note that since the labour hiring problem is static, optimal labour can be obtained independently of next period's optimal capitals k', k'^f given the beginning of period pre-installed stock of capitals. Recall that given our assumption that firms are owned by foreign risk neutral investors the discount factor of the firm is a constant, β .

Therefore, the optimal labour choice for the firm is:

$$n(l, z, k, k^f; \mathbf{S}) = \left(\frac{w(\mathbf{S})}{R(\mathbf{S})z(R(\mathbf{S})k)^{\alpha\mu}(1-\alpha)\mu} \right)^{\frac{1}{(1-\alpha)\mu-1}} \tag{7}$$

Clearly, those areas hit by a flood a_l will experience lower labour demand as their productive capability will be hindered in the form of a reduced stock of capital and production frontier for the period.

Optimality for the production capital requires:

$$\begin{aligned}\frac{\partial V}{\partial k'} = & -1 - \text{convex cost term} \\ & + \beta \mathbf{E} \left(R'(\mathbf{S}')^{1+\alpha\mu} z' \alpha \mu (k')^{\alpha\mu-1} n'^{\mu(1-\alpha)} \right. \\ & \quad \left. + (1-\delta)R'(\mathbf{S}') + \text{convex cost terms} \right)\end{aligned}\tag{8}$$

Which is the standard optimality condition relating the cost of the additional capital in the current period relative to the marginal product of capital and resale value in the next period. The difference is that, compared to the standard model, with flood risk only a fraction $R'(S')$ will be operable in the next period. This fraction, in turn, will depend on the choice of the flood preventing capital:

$$\begin{aligned}\frac{\partial V}{\partial k^{f'}} = & -1 - \text{convex cost term} \\ & + \beta \mathbf{E} \left[\begin{aligned} & (1 + \alpha\mu) R'(S')^{\alpha\mu} z' \left(k'^{\alpha} n'^{(1-\alpha)} \right)^{\mu} F'(k^{f'}) \mathbb{I}_{a_{l'}=1} \\ & + (1 - \delta) k' F'(k^{f'}) \mathbb{I}_{a_{l'}=1} \\ & + (1 - \delta) k^{f'} F'(k^{f'}) \mathbb{I}_{a_{l'}=1} \\ & + (1 - \delta) R'(S') \\ & + \text{convex cost terms} \end{aligned} \right]\end{aligned}\tag{9}$$

This first order condition acts through two channels. First, as with the standard production capital, acquiring more flood preventing capital today will lead to a higher resale value tomorrow $(1 - \delta)R'(S')$. Secondly, and crucially, accumulating flood preventing capital will increase the fractions of production and capital stocks that are retained in the event of a flood, $\mathbb{I}_{a_{l'}=1}$.

Therefore, the key determinants of whether it is optimal for the firms to invest in the flood preventing capital are (i) the probability that a flood will happen in the next period, given by the Markov Process Γ_l and (ii) the marginal gains of investing on flood preventing capital on the retained fraction of production and capital $\frac{\partial F(k^f)}{\partial k^f}$. Note that under no flood risk the optimal amount of flood preventing capital would be nought as the cost of acquiring the capital would dominate the expected depreciated value thereof.

3.3 Household Optimization

Given the simplifying assumptions of (i) firms being owned by risk-neutral foreign investors (ii) no mobility across regions and (iii) GHH preferences, the problem of the households is straightforward:

$$\begin{aligned} & \max_{C,N} \log(C - \xi \frac{N^{1+\eta}}{1+\eta}) \\ & s.t. \quad C \leq w(\mathbf{S})N \end{aligned} \tag{10}$$

Which results in the static labour supply equation:

$$N = \left(\frac{w(\mathbf{S})}{\xi} \right)^{\frac{1}{\eta}} \tag{11}$$

3.4 Equilibrium Definition

A Recursive Competitive Equilibrium (RCE) of this economy is a set of policy functions $k^f(l, z, k, k^f; \mathbf{S})$, $k'(l, z, k, k^f; \mathbf{S})$, $n(l, z, k, k^f; \mathbf{S})$, value function $V(l, z, k, k^f; \mathbf{S})$, labour supply $N(\mathbf{S})$, prices $w(\mathbf{S})$ and r , and invariant distribution $\mu(l, z, k, k^f)$ such that:

- Given prices, the policy function $N(\mathbf{S})$ solves the households' labour supply problem.
- Given prices, state of the economy \mathbf{S} and invariant distribution $\mu(l, z, k, k^f)$, the policy functions $k^f(l, z, k, k^f; \mathbf{S})$, $k'(l, z, k, k^f; \mathbf{S})$, $n(l, z, k, k^f; \mathbf{S})$ and value function $V(l, z, k, k^f; \mathbf{S})$ solve the firms' problem.
- The invariant distribution μ satisfies:

$$\mu(L \times Z \times K \times K^f) = \int T((l, z, k, k^f), L \times Z \times K \times K^f) d\mu(l, z, k, k^f) \forall L \subset \mathcal{L}, Z \subset \mathcal{Z}, K \subset \mathcal{K}, K^f \subset \mathcal{K}^f \tag{12}$$

Where $T(\cdot)$ is the transition function defined as:

$$T((l, z, k, k^f), L \times Z \times K \times K^f) = \mathbb{I}_{k'(l, z, k, k^f; \mathbf{S}) \in L} \mathbb{I}_{k^f(l, z, k, k^f; \mathbf{S}) \in K^f} \sum_{z' \in Z} \pi_z(z, z') \mathbb{I}_{l \in L} \tag{13}$$

Where recall that firms are immobile across locations and $\pi_z(z, z')$ is the p.d.f. of the idiosyncratic shocks z .

- The demand and supply for labour is clared at every aggregate state \mathbf{S} at prices $w(\mathbf{S})$:

$$L_l \left(\frac{w(\mathbf{S})}{\xi} \right)^{\frac{1}{\eta}} = \int n(l, z, k, k^f; \mathbf{S}) d\mu \quad \text{at each } l \tag{14}$$

4 Calibration and Solution Method

The present section discusses the calibration and employed solution methodology.

4.1 Calibration

This preliminary draft closely follows standard values in the literature in order to aid with the validation of the solution method. In particular, we largely follow the quarterly calibration in [Winberry \(2021\)](#) for the standard parameters, and discuss the calibration of the model specific features in greater detail shortly.

Fixed Parameters Overall, we set the time horizon to a quarter. Subsequently, the chosen discount factor β is 0.99, implying a quarterly 1% interest rate. On the household side, the Frisch elasticity $\frac{1}{\eta}$ is set to 2.0 and the disutility of labour ξ is set to 2.1.

On the firm side, first, a depreciation rate of 2% is chosen, so that the approximate yearly depreciation rate is 8%. Second, the returns to scale μ are set to 0.8, a common value in the literature. Third, the share of capital in production α is set to 0.36, again a standard value in the literature, and that of labour to 0.64. Lastly, the process for the idiosyncratic productivity shocks z is set so that the autocorrelation is $\rho_z = 0.9$ and the standard deviation $\sigma_z = 0.053$, as estimated in [Winberry \(2021\)](#). Lastly, the convex costs ϕ are set to 0.02, a relatively low value in the literature but sufficient to generate a continuous distribution of investment rates. The parameters are shown in table 2.

Table 2: Fixed Parameters in the Model.

Parameter	Definition	Value
Time Horizon β	Discount Factor	0.99
Household Block η ξ	Inverse Frisch Elasticity Disutility of Labour	0.5 2.1
Firm Block δ μ α ρ_z σ_z ϕ	Depreciation Rate Returns to Scale Capital Share Production Autocorrelation Idiosyncratic Shocks Volatility Idiosyncratic Shocks Convex Costs	0.02 0.8 0.36 0.9 0.053 0.02

Model-specific parameterization

While the model is embedded within a standard firm dynamics setting à la [Khan and Thomas \(2008\)](#), there are two main features specific to our setting, namely the Markovian Process for the flood risk per location, Γ_l , and the function regulating the strength of the flood preventing capital, $F(k^f)$.

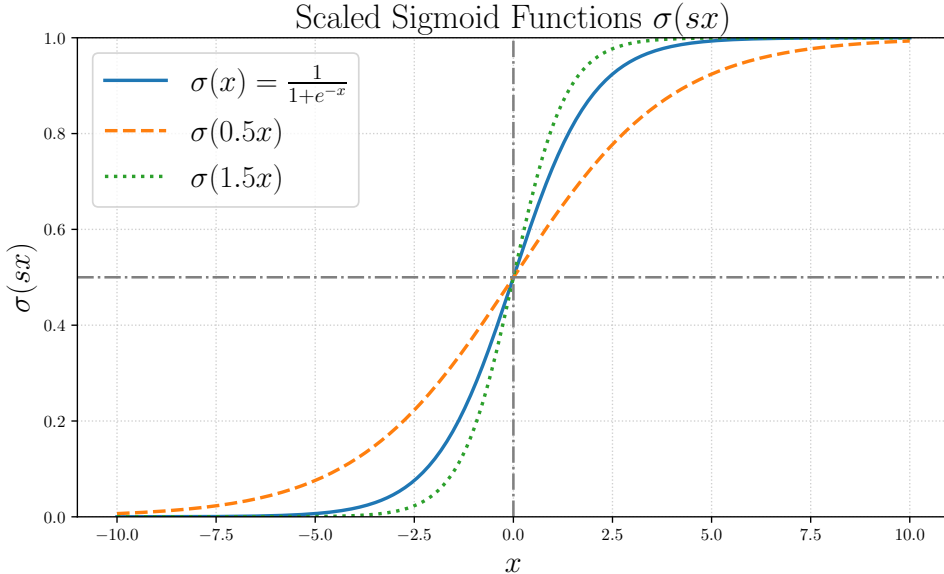
First, regarding the flood risk processes $\{\Gamma_l\}_{l=1}^L$, we assume the existence of two locations, Safe and Risky, each with their own process. We assume that the population is split equally among the two locations, and, based on the occurrence of floods during the sample period in the data, we assign a flood probability of 6% to the Safe area and a 14% one to the Risky area, which corresponds to floods occurring every 16 and 7 quarters, respectively. Thus, the Markovian Chains read as follows:

$$\Gamma_{\text{Safe}} = \begin{bmatrix} 0.94 & 0.06 \\ 0.94 & 0.06 \end{bmatrix} \quad \Gamma_{\text{Risky}} = \begin{bmatrix} 0.86 & 0.14 \\ 0.86 & 0.14 \end{bmatrix} \quad (15)$$

The states are, respectively, $a_l \in \{\text{No Flood}, \text{Flooded}\}$. Note that the probabilities are assumed to be *i.i.d.*; a given realization is not informative about future realizations.

Secondly, there is the function regulating the strength of the flood preventing capital in mitigating damages to both the output and capital stock, $F(k^f)$. We choose the *scaled sigmoid* function $F(k^f) = \frac{1}{1+\exp(-sx)}$ where $s > 0$ is the scaling parameter. This function satisfies the three conditions stated above. Namely, it is bounded between $0 < \frac{1}{1+\exp(-sx)} < 1$, it is increasing, and it is concave in our domain of interest, $k^f \in \mathbf{R}_+$. Furthermore, the scale parameter s allows us to calibrate the marginal benefit from employing an additional unit of flood preventing capital. Figure 4 shows precisely this.

Figure 4: Scaled Sigmoid Function



Notes: Scaled Sigmoid Function employed as the Flood Impact Mitigating Function $F(k^f)$ in the Calibration. The Scale Parameter s regulates the marginal benefit of installing an additional unit of flood preventing capital.

Given that the derivative of the scaled sigmoid function is $\frac{\partial F(k^f)}{\partial k^f} = \sigma(sx)(1 - \sigma(sx))s$, the saturation point where the share of protected output and capital stock is close to 1 is smaller the larger s is. In other words, for a given desired protection level by the firm

$p \in (0.5, 1)$, a lower level of stock of flood preventing capital will be required the larger s is. This preliminary draft employs a value of $s = 1$, which collapses to the standard sigmoid function and as we shall see in the next section implies a plausible ratio between the flood preventing and production capitals.

4.2 Solution Method

There are three main challenges to solve this model. First, we have the presence of both idiosyncratic and aggregate uncertainty. Second, the dimensionality of the state space in the full model can be quite large, with L states of flooding, L prices $W_l(\mathbf{S})$ and the entire distribution $\lambda(l, z, k, k^f)$ to be accounted for. Third, prices are not cleared within period in a straightforward manner due to the presence of heterogeneous firms, and solving for prices as a function of the aggregate state \mathbf{S} is required.

To overcome said challenges, we employ the methodology proposed in [Maliar et al. \(2021\)](#) and [Han et al. \(2021\)](#), which relies on utilizing deep learning techniques. The advantages of employing deep learning as opposed to grid-based methods are mainly threefold. First, while a grid discretization scaled non-linearly with the number of dimensions, training Neural Networks (NN henceforth) requires data sampling, which for a given data size scales linearly in the number of dimensions. Note that this is already a game changer: a model with 30 dimensions and 5 grid points per dimension would require 9.31e20 elements in total, whereas a sampling method requires $30 \times N$, with N being the number of samples. Furthermore, the ability to train the NN employing *batches*, a subset of the data, guarantees that memory consumption remains manageable.

Secondly, as we shall discuss briefly, the embedded sampling methodology in the algorithm guarantees that the training data is drawn from the ergodic set where the solution “lives”. This is crucial, as opposed to a grid-based method, the accuracy is where it is needed, not uniformly along the entire hypercube. As outlined in [Maliar et al. \(2021\)](#), if we assume that the ergodic set of the model is a hypersphere of diameter 1, the ratio of the volume of the hypersphere relative to that of the cube decreases exponentially as the dimensionality increases. With two dimensions, $d = 2$, the ratio is 79%, but this falls quickly to 2×10^{-14} for at $d = 30$. Therefore, the accuracy of a grid-based hypercube quickly falls as the number of dimensions increases relative to a simulation-based approach.

Third, NNs have been shown to be universal approximators. In particular, it can be shown that any continuous function with domain on an n-dimensional hypercube can be approximated by a NN with sufficient width and just one layer ([Cybenko, 1989](#)). A key condition is that the employed activation functions in the hidden layers are not polynomial, as this family has limited ability to capture arbitrary relationships ([Hornik et al., 1989](#)). In economics, this translates into the guarantee that either the policy functions or value functions will be approximated correctly by a sufficiently wide NN.

The algorithm that we implement 1 closely follows the one in [Han et al. \(2021\)](#), with the addition of multiple controls and an auxiliary NN for the market clearing prices $w(\mathbf{S})$, which need to clear labour supply and demand at every region and aggregate state \mathbf{S} . The implementation is done with Pytorch and is compiled via TorchScript. Further details are provided in the appendix [\(7\)](#).

Algorithm 1 DeepHam Han et al. (2021)-based algorithm for the model economy.

- 1:
- 2: Step 0. Initialize the production capital, flood preventing capital, value function and wage NNs, $K_{NN}^0(\Theta)$, $K_{NN}^{f,0}(\Theta)$, $V_{NN}^0(\Theta)$, $w_{NN}^{l,0}(\Theta)$. Fix the number of agents in the economy, N , and the number of economies to be simulated, E .
- 3:
- 4: Pre-training. Perform a preliminary learning via regression so that the production capital and flood preventing capital NNs output the steady-state level of capital k_{ss} . Likewise, pre-train the wage NN to learn the steady-state value w_{ss} .
- 5:
- 6: **for** $k = 1, 2, \dots, k_{max}$ **do** (outer DeepHAM iterations)
- 7:
- 8: Step 1 (Simulation): Obtain the ergodic distribution of the economy $\mu^k(\cdot)$ by simulating the economy forward with the current guesses $K_{NN}^{k-1}(\Theta)$, $K_{NN}^{f,k-1}(\Theta)$ and $w_{NN}^{l,k-1}(\mathbf{S})$.
- 9:
- 10: Step 2 (Training the Value Function $V_{NN}^k(\Theta)$): Draw E initial conditions from the ergodic distribution $\mu^k(\cdot)$ and simulate the shocks forward with $\{\Gamma_l\}_{l=1}^L$ and $\pi(z, z')$. Next, compute the terminal realized value $V^T(\cdot)$ on these Monte Carlo paths by simulating forward the economy with $K_{NN}^{k-1}(\Theta)$, $K_{NN}^{f,k-1}(\Theta)$ and $w_{NN}^{l,k-1}(\mathbf{S})$. Lastly, train $V_{NN}^k(\Theta)$ to learn these terminal realized values:

$$\min_{\Theta^V} \mathbf{E}_{\mu^k(\cdot), z, a_l}_{l=1}^L \left(V_{NN}^k(\Theta) - V^T(\cdot) \right)^2$$

- 11:
- 12: Step 3 (Training the policy functions $K_{NN}^k(\Theta)$, $K_{NN}^{f,k}(\Theta)$ and $w_{NN}^{l,k}(\mathbf{S})$): As in Step 2, draw E initial conditions from the ergodic distribution $\mu^k(\cdot)$ and simulate the shocks forward with $\{\Gamma_l\}_{l=1}^L$ and $\pi(z, z')$. Build the computational graph associated with the economy, and simulate it forward. At each evaluation, $K_{NN}^k(\Theta)$, $K_{NN}^{f,k}(\Theta)$ are updated via Stochastic Gradient Descent to optimize:

$$\max_{\Theta^K, \Theta^{K^f}} \mathbf{E}_{\mu^k(\cdot), z, a_l}_{l=1}^L \left(\sum_{t=0}^{t=T-1} \beta^t \pi_i(\cdot) + \beta^T V_{NN}^k(\Theta) \right)$$

While $w_{NN}^{l,k}(\Theta)$ is trained to minimize:

$$\min_{\Theta^W} \mathbf{E}_{\mu^k(\cdot), z, a_l}_{l=1}^L \left(\sum_{t=0}^{t=T-1} \sum_{l=1}^L L_{d,t,l}(\cdot) - L_{s,t,l}(\cdot) \right)^2$$

Where $L_{d,t,l}$ is aggregate labour demand at time t in location l and $L_{s,t,l}$ is the labour supply counterpart.

- 13:
 - 14: **end for**
-

5 Results

This section presents the main results of the paper. The empirical section provided a key stylized fact arguing that historically less exposed areas experienced larger production and capital stock losses following a flood, relative to their counterparts with higher historical exposure. To rationalize this finding, we proposed a firms dynamics model with aggregate flood uncertainty that allowed for investment in a distinct type of capital, the flood preventing capital. The core functionality of this capital was to insure privately the output and capital stocks of a firm in the event of a flood.

Is adaptation through investment in the flood preventing capital consistent with the empirical findings? What are its implications for the ergodic distribution of investment of each type of capital in safer and riskier areas? In this section, we proceed in two steps. First, we study the predictions of the model mechanisms regarding the ergodic distribution of both capitals across space and capital types. Second, we examine the response of the economies in safer and riskier areas to a flood shock, and track the responses of the main aggregates of interest of the economy.

5.1 Ergodic Distributions of Capital across Space and Capital Types

Recall from the model section that we assumed two types of capital: the one employed in production, k , and the flood preventing capital, k^f . The former follows the standard rationale in macroeconomics: an investment cost in the current period of one unit of the final good provides certain increased production and resale value in the next. The latter operates differently. While the investment cost today is the same, the returns to the investment vary as a function of the exposure to flood risk. Upon a flood shock, this capital mitigates the damages to both production and the capital stock, in a marginally decreasing fashion.

Therefore, intuitively, we would expect locations with higher exposure to flood risk to invest more heavily in the flood preventing capital technology, as the state of the world where the returns to it can materialize takes place with higher probability. A related question is whether the investment need in the flood preventing capital in riskier regions poses a heavy strain on the production capital that the firm is able to operate at.

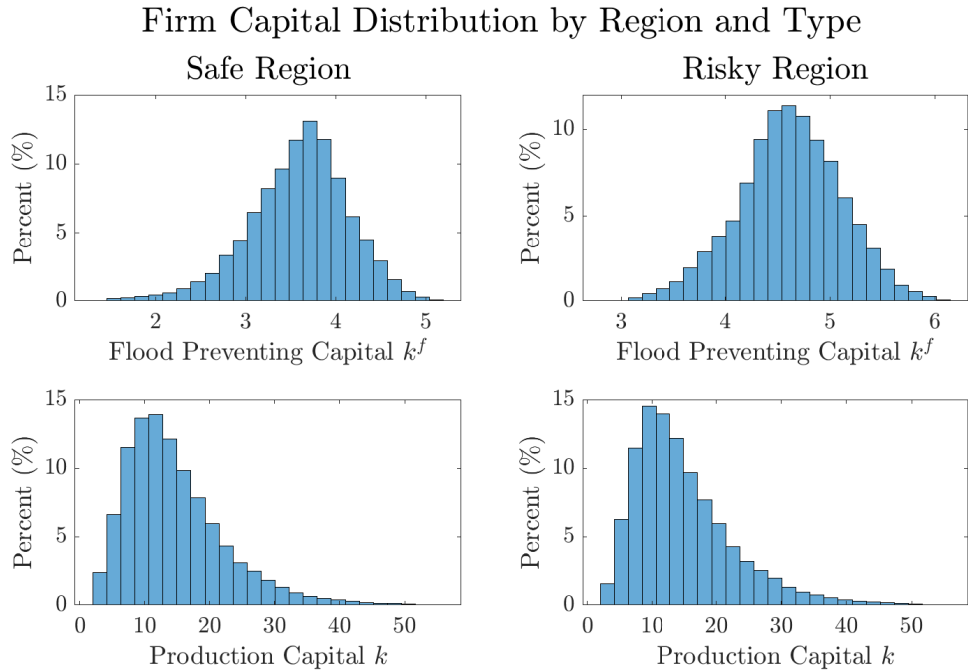
Figure (5) contains the ergodic distributions of firm-level investment in each capital by location type under aggregate flood uncertainty. Results are separated by region, with the left column showing the results for the Safe region and the right column doing so for the Risky region. Furthermore, the top row contains the figures for the flood preventing capital k^f , while the bottom row shows the results for the production capital k .

Two main observations are in place. First, as foretold by the previous discussion, investment in the flood preventing capital is higher in the Risky region, where the quarterly flood probability is about 14%. The average chosen level of investment, of around 4.5, protects the stocks of capital and production at a 98.9% given our sigmoidal choice for the mitigat-

ing function $F(k^f)$. In contrast, the protection level in the Safe region, corresponding to an investment level of around 3.5 units of flood preventing capital is 97.07%, which corresponds to a 6% flood probability. Thus, we obtain a strict ranking of investment in the flood preventing capital as a function of the exposure of the region to this phenomena, in line with the intuition in equation (9).

Second, regarding the investment in the production capital, we find, in this preliminary calibration that the Safe region's investment is stochastically dominated by that of region 1. That is, for any capital level x , the probability that $P(k \leq x)$ is higher in the Safe region. This, however, we interpret as a *local* rather than *global* property. On one hand, the presence of the flood risk leads to a precautionary capital accumulating motive for the firms, particularly when the marginal gains from the investment in the flood preventing capital are high, as in the current calibration. On the other, there is the cost of keeping the stock of flood preventing capital, which weakens the degree to which the optimal scale of production can be maintained. In the appendix 7.2, we show how decreasing the marginal benefit from investing in flood preventing capital $F'(k^f)$ results in this being overturned.

Figure 5: Distribution of Firms' Capital in the Risky Steady State of the Model, by Region and Type



Notes: The Safe Region has a Flood Probability of 6%, while the Risky Region has a 14% probability. The left column contains the data for the Safe Region while the right column contains the data for the Risky Region. The top row shows the Flood Preventing Capital k^f distribution while the bottom one shows the one for the Production Capital k .

5.2 Responses to Flood Shocks across Space

The main empirical finding suggested that regions with high historical exposure to floods experienced a smaller relative decline in production and capital stocks following a flood.

To rationalize this finding, we proposed a firms dynamics spatial model that allowed firms to invest in the flood preventing capital, whose main role was to mitigate the damages generated by floods on both production and capital stocks. In this section, we focus on analyzing whether the proposed mechanism can generate responses consistent with the data.

To this end, we compute the Impulse Responses of both regional economies to an unexpected flood shock and trace the response of the main aggregates of interest over time. Given that the model features no steady-state, we simulate many paths for the economy and compute the average impulse response across simulations:

$$IRF_{t+h} = \frac{1}{N} \sum_{n=1}^N \left(\frac{Y_{l,t+h}(a_{l,t+h} + \mathbb{I}_{h=0}, \mu_{t+h}) - Y_{l,t+h}^*(a_{l,t+h}^*, \mu_{t+h}^*)}{Y_{l,t+h}^*(a_{l,t+h}^*, \mu_{t+h}^*)} \right) \times 100 \quad (16)$$

Where N is the number of economies simulated, Y stands for an aggregate of interest, $\mathbb{I}_{h=0}$ denotes the shock to the flood status at period t , and $\{x^*\}_t^{t+h}$ is a generic sequence without the additional flood shock and $\{x\}_t^{t+h}$ are the shocked counterparts. Figure (6) displays the obtained results.

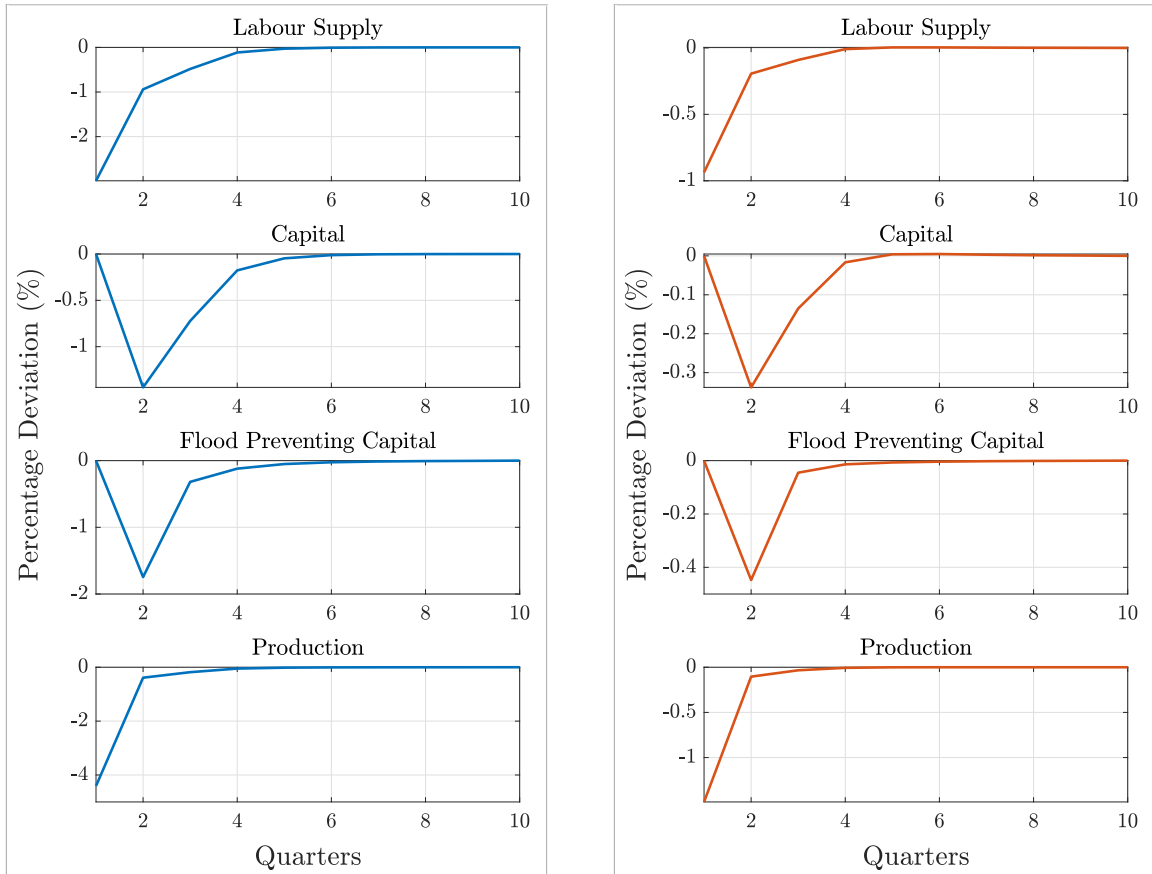
Clearly, following a flood shock (time of impact set to 1 on the x-axis), the response of the aggregates of interest is negative and persistent across both economies. Importantly, however, the responses in the Safe region experience a larger decline than those in the Risky region. This is also the case in the calibration with lower marginal benefits from investing in the flood preventing capital, $F'(k^f)$, 7.3. This is consistent with the main empirical findings, and is driven by the increased incentives to invest in the flood preventing capital in the risky region.

As discussed in the previous section, firms in the Risky region have a protection level against floods of 98.9% on average, as opposed to the 97.07% of those in the Safe region. This directly translates into a larger decline in the capital stock and production in the Safe region in the event of a flood. Upon impact, a fraction $1 - F(K^f)$ of the production y and flood preventing capital stocks k and k^f are lost to the flooding, with the response for output being aggravated by the decreased capital stock.

Inspecting each aggregate separately, we can observe that the decline of labour on impact is around -3% in the Safe region compared to the -1% in the Risky region, and requires about 4 quarters to revert back. The decline in labour demand is a direct result of the decreased labour demand following a reduced capital stock and production frontier when the shock hits.

Regarding the response of capital, since we defined it to be the beginning-of-period one, its response does not appear until period 2, where the decline is of around -1.5% in the Safe region and of around -0.3% in the Risky region. It is important to note here that

Figure 6: IRFs to a Flood Shock, by Region
 Safe Region (Region 0) Risky Region (Region 1)



Notes: Obtained IRFs as a response to a Flood Shock averaged across 1000 starting conditions. The x-axis shows the time horizon, which is set to quarters, and is 1-indexed. The y-axis shows the percentage deviation (%) w.r.t. the risky steady-state. The left column shows the IRFs for the Safe Region, while the right one does so for the Risky Region. Both Capitals are the beginning of period ones.

between t and $t + 1$ the firm has the option to invest in more capital, and consequently the protection level is but a lower bound on its response. Interestingly, the response of the flood preventing capital is more pronounced than that of the production capital, suggesting that firms focus their resources on investing in the production capital first. This is consistent with the FOC for the flood preventing capital [9](#), which states that the benefit of installing an additional unit thereof is greater the higher is the stock of the production capital (positive cross-derivative).

Lastly, production experiences the largest decline on impact. This is due to the combined effect of the decreased stock of production capital and the direct impact of floods on production. The losses increase to -4% in the Safe region and to around -1.5% in the Risky region. In the case of the Safe region, it exceeds the protection level's 97.07% buffer given the aforementioned combined effect.

In summary, upon an unexpected flood shock, the Safer region, where the investment in the stock of the flood preventing capital is lower, experiences larger declines across all of the analyzed aggregates of interest. Taken together, the results from the previous and present section point to a noteworthy implication of exposure to flood risk; while the average profits across time are lower in the riskier region, investment in alleviating the damages implies that in the event of a flood the disturbance will be lower, and the recovery faster, than in the safer region.

6 Conclusion

In this paper, we studied how manufacturing firms in India adapt to the ever increasing risk of extreme climate events, in particular to flooding. Employing rich establishment-level data from the Annual Survey of Industries (ASI) in conjunction with flood event data from the Dartmouth Flood Observatory (DOF) and the state-of-the-art methodology by [De Chaisemartin and d'Haultfoeuille \(2024\)](#), we found empirical evidence pointing to establishments in historically less exposed districts experiencing larger declines in their production and capital following a flood.

To rationalize these findings, we proposed a firm dynamics dynamic spatial model. In the model, locations were heterogeneous in their probability of experiencing a flood, and firms were able to invest in a flood preventing capital that mitigated the damages caused by flooding to both capital and production. Given the setup with aggregate uncertainty and the requirement for agents to keep track of prices across space and time under rational expectations, the usage of deep learning techniques was required in order to tame the curse of dimensionality.

We then took this model to a two-region calibration with flood probabilities estimated from the data. We found that at the risky-steady state establishments in the Risky Region invested more in flood preventing capital, which negatively affected their discounted sum of

profits relative to their counterparts in the Safer Region. We then computed the responses in each region to a flood shock, and found that the flood preventing capital accumulation mechanism was able to rationalize the findings in the data. In particular, we found that following a flood shock all of the aggregates of interest (including capital and production) experienced a larger decline in the Safer Region, due to their lower investment in this adaptation mechanism.

There are however interesting avenues for future research. First, finding empirical support for the spatial differences in the investment of flood preventing capital would be crucial, as well as identifying this type of capital in the data. Second, a realistic calibration, capable of replicating key moments and spatial characteristics of the Indian economy would be crucial in order to perform sound policy exercises. Third, while we currently only consider private insurance against flooding, the public sector could play a key role, and subsidies could potentially help explain why capital and production in areas with high historical exposure experience a positive response in the data.

References

- ALBERT, C., P. BUSTOS, AND J. PONTICELLI (2024): "The Effects of Climate Change on Labor and Capital Reallocation," Tech. rep. 4
- AZINOVIC, M., L. GAEGAUF, AND S. SCHEIDECKER (2022): "Deep equilibrium nets," *International Economic Review*, 63, 1471–1525. 4
- BALBONI, C. (2025): "In harm's way? infrastructure investments and the persistence of coastal cities," *American Economic Review*, 115, 77–116. 3
- BALBONI, C., J. BOEHM, AND M. WASEEM (2024): "Firm adaptation in production networks: evidence from extreme weather events in pakistan Mimeo," . 4
- CASTRO-VINCENZI, J. (2024): "Climate Hazards and Resilience in the Global Car Industry," Ph.D. thesis, Princeton. 4, 9, 10
- CASTRO-VINCENZI, J., G. KHANNA, N. MORALES, AND N. PANDALAI-NAYAR (2024): "Weathering the storm: Supply chains and climate risk," Tech. rep., National Bureau of Economic Research. 4
- CYBENKO, G. (1989): "Approximation by superpositions of a sigmoidal function," *Mathematics of control, signals and systems*, 2, 303–314. 21
- DE CHAISEMARTIN, C. AND X. D'HAUTFOUEUILLE (2023): "Two-way fixed effects and differences-in-differences with heterogeneous treatment effects: a survey," *The Econometrics Journal*, 26, C1–C30. 9
- DE CHAISEMARTIN, C. AND X. D'HAUTFOUEUILLE (2024): "Difference-in-differences estimators of intertemporal treatment effects," *Review of Economics and Statistics*, 1–45. 4, 9, 10, 11, 28
- DESMET, K., R. E. KOPP, S. A. KULP, D. K. NAGY, M. OPPENHEIMER, E. ROSSI-HANSBERG, AND B. H. STRAUSS (2021): "Evaluating the Economic Cost of Coastal Flooding," *American Economic Journal: Macroeconomics*, 13, 444–86. 3
- FICARRA, M. AND R. MARI (2025): "Weathering the storm: sectoral economic and inflationary effects of floods and the role of adaptation," . 4
- FRIED, S. (2022): "Seawalls and stilts: A quantitative macro study of climate adaptation," *The Review of Economic Studies*, 89, 3303–3344. 4
- GANDHI, S., M. E. KAHN, R. KOCHHAR, S. LALL, AND V. TANDEL (2022): "Adapting to flood risk: Evidence from a panel of global cities," Tech. rep., National Bureau of Economic Research. 4
- GIANNONE, E., Q. LI, N. PAIXAO, AND X. PANG (2020): "Unpacking moving," *Unpublished manuscript*. 13
- GREENWOOD, J., Z. HERCOWITZ, AND G. W. HUFFMAN (1988): "Investment, capacity utilization, and the real business cycle," *The American Economic Review*, 402–417. 15
- HAN, J., Y. YANG, ET AL. (2021): "Deepham: A global solution method for heterogeneous agent models with aggregate shocks," *arXiv preprint arXiv:2112.14377*. 4, 21, 22, 23, 32, 33
- HORNIK, K., M. STINCHCOMBE, AND H. WHITE (1989): "Multilayer feedforward networks are universal approximators," *Neural networks*, 2, 359–366. 21
- HOSSEIN, F. (2020): "Creative Destruction or Just Destruction? Effects of Floods on Manufacturing Establishments in India," *Working Paper*. 3
- JIA, R., X. MA, AND V. W. XIE (2025): "Expecting Floods: Firm Entry, Employment, and Aggregate Implications," *American Economic Journal: Macroeconomics*, Forthcoming. 3
- KAHOU, M. E., J. FERNÁNDEZ-VILLAVERDE, J. PERLA, AND A. SOOD (2021): "Exploiting symmetry in high-dimensional dynamic programming," Tech. rep., National Bureau of Economic Research. 4
- KHAN, A. AND J. K. THOMAS (2008): "Idiosyncratic shocks and the role of nonconvexities in plant and aggregate investment dynamics," *Econometrica*, 76, 395–436. 3, 13, 14, 19
- KLEINMAN, B., E. LIU, AND S. J. REDDING (2023): "Dynamic spatial general equilibrium," *Econometrica*,

91, 385–424. 13

KRUSELL, P. AND A. A. SMITH, JR (1998): “Income and wealth heterogeneity in the macroeconomy,” *Journal of political Economy*, 106, 867–896. 4

MALIAR, L., S. MALIAR, AND P. WINANT (2021): “Deep learning for solving dynamic economic models.” *Journal of Monetary Economics*, 122, 76–101. 4, 21

MARTIN, L. A., S. NATARAJ, AND A. E. HARRISON (2017): “In with the big, out with the small: Removing small-scale reservations in India,” *American Economic Review*, 107, 354–86. 5

NATIONAL DISASTER MANAGEMENT AUTHORITY, GOVERNMENT OF INDIA (2023): “Floods,” <https://ndma.gov.in/Natural-Hazards/Floods>, accessed: 2025-05-09. 2

PANG, X. AND P. SUN (2024): “Moving into Risky Floodplains: the Spatial Implication of Flood Relief Policies,” . 3, 4

PANKRATZ, N. M. AND C. M. SCHILLER (2024): “Climate change and adaptation in global supply-chain networks,” *The Review of Financial Studies*, 37, 1729–1777. 4

PELLI, M., J. TSCHOPP, N. BEZMATERNYKH, AND K. M. EKLOU (2023): “In the eye of the storm: Firms and capital destruction in India,” *Journal of Urban Economics*, 134, 103529. 3

PÖRTNER, H.-O., D. C. ROBERTS, H. ADAMS, C. ADLER, P. ALDUNCE, E. ALI, R. A. BEGUM, R. BETTS, R. B. KERR, R. BIESBROEK, ET AL. (2022): “Climate change 2022: Impacts, adaptation and vulnerability,” *IPCC Sixth Assessment Report*, 37–118. 2

RAO, S., S. KOIRALA, C. THAPA, AND S. NEUPANE (2022): “When rain matters! Investments and value relevance,” *Journal of Corporate Finance*, 73, 101827. 3

SOMANATHAN, E., R. SOMANATHAN, A. SUDARSHAN, AND M. TEWARI (2021): “The impact of temperature on productivity and labor supply: Evidence from Indian manufacturing,” *Journal of Political Economy*, 129, 1797–1827. 4

WINBERRY, T. (2021): “Lumpy investment, business cycles, and stimulus policy,” *American Economic Review*, 111, 364–396. 13, 19

7 Computational Appendix

In this section we provide additional details on the employed environment and setup, hyperparameter configuration and structure of the NNs.

7.A Environment and Setup

The implementation is written in Pytorch 2.7. There are two main reasons for this. First, as opposed to Tensorflow, Pytorch can be installed locally on a Windows 10/11 machine to utilize a dedicated GPU without any further requirements⁶. Second, Pytorch 2.0+ allows for convenient compilation of the code through either the `torch.compile()` or `torch.jit.script()` APIs. In addition to this, Pytorch's eager execution runs line by line as standard Python, therefore debugging is seamless.

Pytorch 2.0+ supports GPU hardware acceleration on multiple backends, most notably CUDA⁷ and MPS⁸. It is also compatible with Vulkan and OpenCL at an experimental state, allowing for the use of GPUs of other brands (AMD). It is most mature at CUDA however, thanks to its established cuDNN (Deep Learning primitives) and cuBLAS (Algebra primitives) libraries as well as the availability of Tensor Cores at the hardware level on Nvidia's GPUs. Usage of Pytorch 2.0+ with CUDA requires the availability of an Nvidia GPU with the relevant compute capability (CC), the CUDA Toolkit and the associated Graphics Drivers. Conveniently, Google Colab provides the researcher with a plug-and-play experience to run the Pytorch 2.0+ code on a GPU thanks to the availability of the GPU-T4 environment.

The core functionality of these Deep Learning frameworks is to allow us to cast our dynamic programming problem into a differentiable *computational graph* where the derivatives of the loss / objective function with respect to the Neural Network parameters can be computed. This allows us to find the optimal Θ^* such that the attained discounted sum of profits by the firms is the highest and the local labour markets clear as tightly as possible.

7.B Hyperparameter tuning (Algorithmic and Architectural)

A key margin for the reproducibility of Deep Learning applications is the choice for the *hyperparameters* that govern the underlying training process. These include, for example, the learning rates, batch sizes, hidden layer activation functions, ... Table (7.1) provides the entire set of hyperparameters in our implementation.

Regarding the structure of the Neural Networks, we opt for relatively shallow NNs of 2 layers and 32 neurons each. This is comparable to the choice in the original paper [Han et al.](#)

⁶Tensorflow requires employing the WSL 2 (Windows Subsystem for Linux) in order to utilize the local GPU.

⁷CUDA (Compute Unified Device Architecture) is Nvidia's proprietary GPU parallel computing platform.

⁸MPS (Metal Performance Shaders) is Apple's proprietary framework for GPU accelerated computing.

Table 7.1: Set of hyperparameters and state space in the Model's Deep Learning [Han et al. \(2021\)](#) implementation.

Hyperparameter / State Space	Definition	Value
Neural Network Architecture		
L	Layers per NN (depth)	2
N_l	Neurons per Layer (width)	32
$\sigma()$	Hidden Layers Activation Function	RELU, $\max(0, x)$
$w_{NN}(\Theta)_{\sigma()}$	Wage PF Output Layer	Softplus, $\log(1 + \exp^x)$
$k_{NN}(\Theta)_{\sigma()}$	Production Capital PF Output Layer	Softplus $\log(1 + \exp(x))$
$k_{NN}^f(\Theta)_{\sigma()}$	Flood Preventing Capital PF Output Layer	Softplus $\log(1 + \exp(x))$
$V_{NN}(\Theta)_{\sigma()}$	Value Function Output Layer	Linear x
Optimizer Settings		
Opt	Optimizer	Adam, AdamW
lr	Learning Rate	$1e - 3$ (PF) and $1e - 4$ (VF)
β_1, β_2	Momentum and Variance of Gradients Parameters	(0.99, 0.999)
Training Settings (DeepHAM)		
E_3	Batch size step 3	150
E_2	Batch size step 2	500
E_1	Batch size step 1	1
e_2	Steps training step 2	3000
e_3	Steps training step 3	75
e_{outer}	DeepHAM Steps (1+2+3)	100
Step 1 Details		
$t_{burn-in}$	Burn-in period simulation	7000
T	Periods Simulated	10000
Step 2 Details		
T_v	Periods simulation for Terminal Value	600
Step 3 details		
T_{pf}	Periods simulation Computational Graph	150
State Space		
0	Location	
1	Idiosyncratic Productivity	
2	Flood Preventing Capital k^f	
3	Production Capital k	
4	Flood Status Safe Region	
5	Flood Status Risky Region	
6	Aggregate Flood Preventing Capital, Safe Region	
7	Aggregate Flood Preventing Capital, Risky Region	
8	Aggregate Production Capital, Safe Region	
9	Aggregate Production Capital, Risky Region	
10	Std. Flood Preventing Capital, Safe Region	
11	Std. Flood Preventing Capital, Risky Region	
12	Std. Production Capital, Safe Region	
13	Std. Production Capital, Risky Region	

(2021) and is the traditionally employed depth in reinforcement learning. We employ a ReLU hidden layers given that their gradients do not saturate and favour sparsity. Regarding the output layers, since our policy function outputs (wages, capitals) are constrained to be on $x \in (0, \infty)$ we employ a *Softplus* output function which matches this range, and whose gradients don't saturate.

As for the optimizer, we employ Pytorch's Adam. Compared to a vanilla SGD, Adam exploits the advantages from momentum β_1 and adaptive learning rates β_2 . Since it computes these moments at a per-parameter basis, it organically controls for gradient magnitudes across layers and parameters.

7.C Validation of the Methodology

To test and validate the accuracy of the proposed solution method and hyperparameter tuning, we compare the ergodic distribution of both the flood preventing and production capitals against a standard grid-based solution.

To isolate the price learning rule, which we can not disentangle from the NN policy functions, we focus on a stationary version of the model without flood risk. While restrictive, note that from the perspective of the DeepHAM methodology, aggregate states are just an additional dimension on which to learn the optimal policy functions, therefore there is no fundamental difference in the learning process for the stationary economy relative to the one under aggregate uncertainty, which is an added benefit of the methodology.

We keep the calibration exactly the same as in (2), the only exception being that we shut down the aggregate flood uncertainty. The results from both methodologies (Deep Learning and Traditional Grid-based) are provided in figure (7.1).

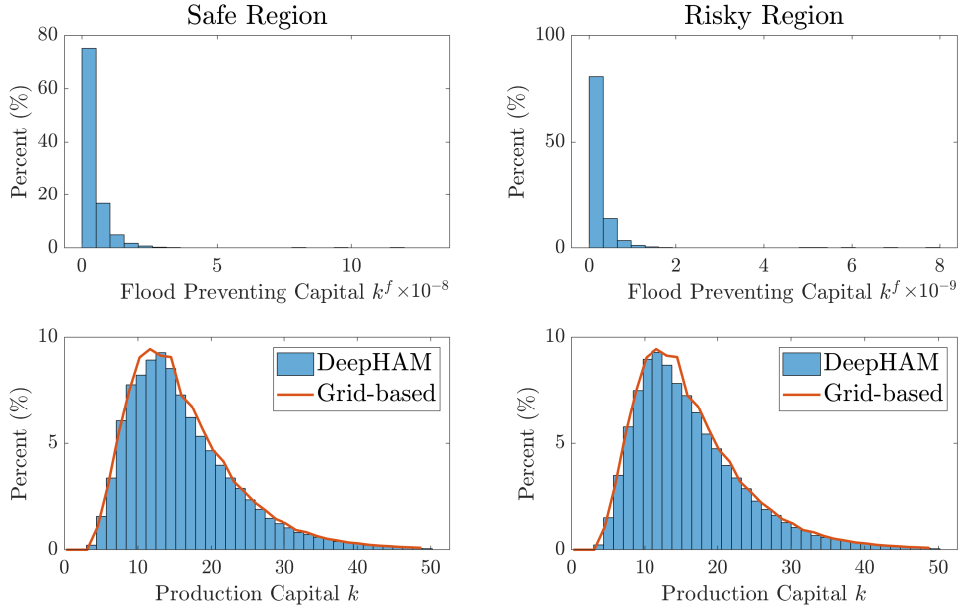
The Deep Learning methodology's solution attains two key merits. First, it properly predicts that investment in the flood preventing capital will be zero in the steady-state economy without flood risk. Second, it is able to replicate the solution attained through standard grid-based solution method for the case of the production capital. This is a robust test given that it is not possible to replicate the ergodic distribution over individual states unless the policy function is accurate over the entire domain.

Therefore, while not exhaustive, this first validation exercise provides reassurance that the employed methodology is sensible and can replicate those attained through standard methods.

7.D Lower Marginal Benefit from Investing in the Flood Preventing Capital $F'(k^f)$

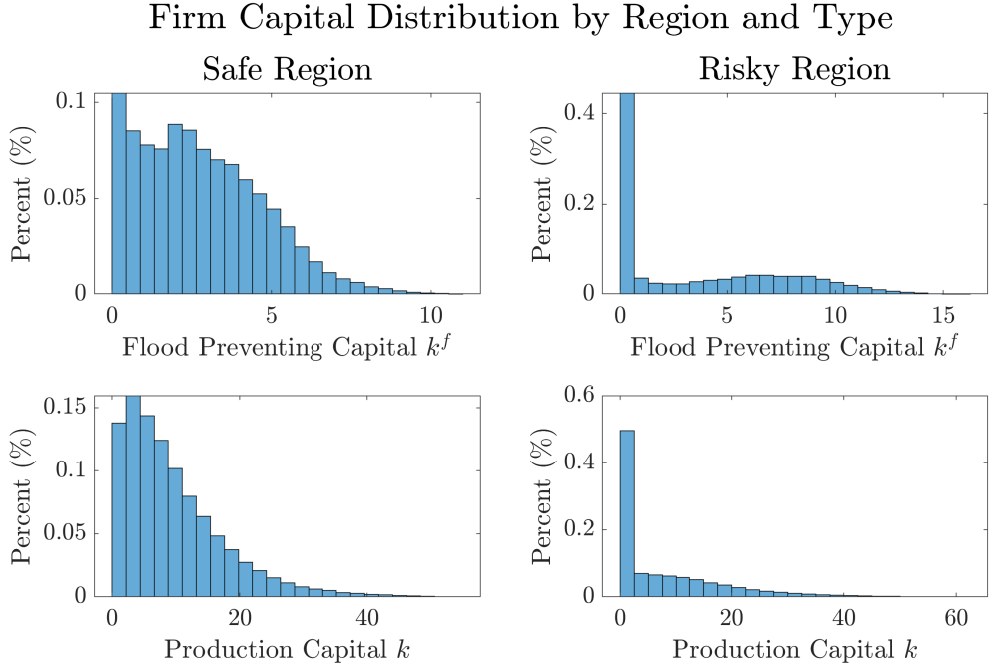
Figure 7.1: Ergodic Distributions of Flood Preventing and Production Capitals under both methodologies.

Validation: Steady-State Firm Capital Distribution by Region and Type



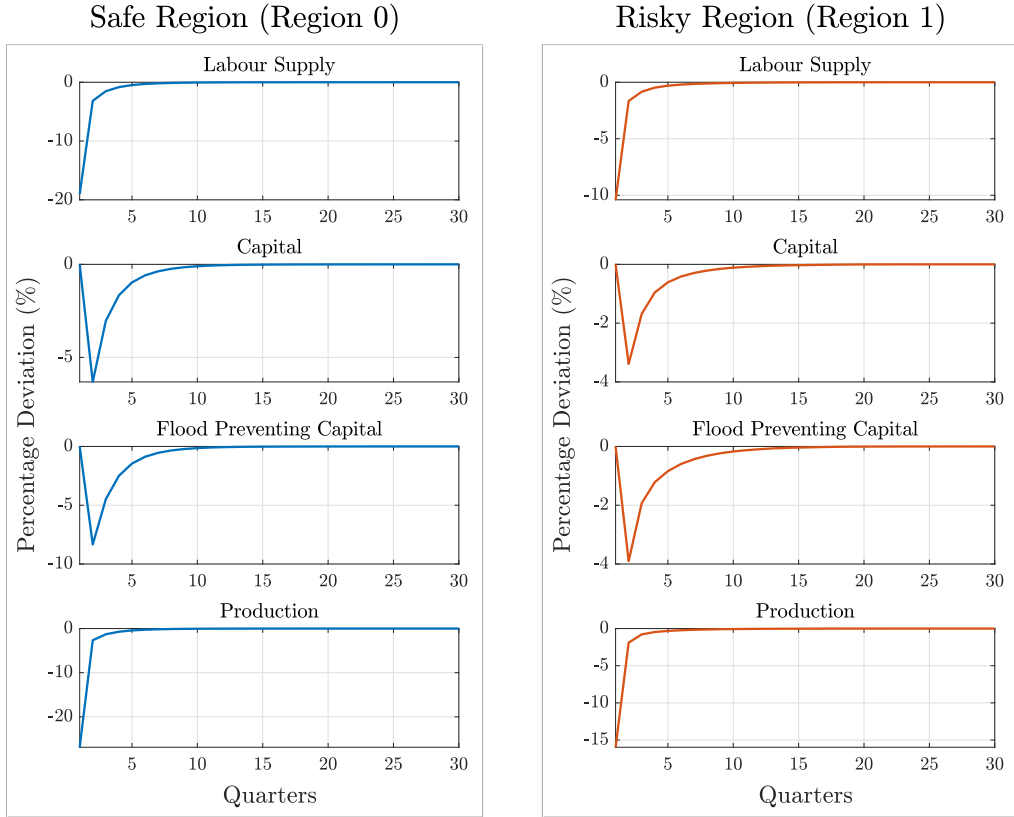
Notes: Steady-state distributions of flood preventing capital (top row) and production capital (bottom row). The bottom row shows the results under standard grid-based methods (VFI, orange) and DeepHAM (blue).

Figure 7.2: Ergodic Distributions of Production and Flood Preventing Capitals under Lower Marginal Benefits $F'(k^f)$



Notes: The Safe Region has a Flood Probability of 6%, while the Risky Region has a 14% probability. The left column contains the data for the Safe Region while the right column contains the data for the Risky Region. The top row shows the Flood Preventing Capital k^f distribution while the bottom one shows the one for the Production Capital k . The parameteric form for the $F(k^f)$ function is now $1 - \exp(-x^{0.6})$

Figure 7.3: IRFs under Lower Marginal Benefits $F'(k^f)$



Notes: Obtained IRFs as a response to a Flood Shock averaged across 1000 starting conditions. The x-axis shows the time horizon, which is set to quarters, and is 1-indexed. The y-axis shows the percentage deviation (%) w.r.t. the risky steady-state. The left column shows the IRFs for the Safe Region, while the right one does so for the Risky Region. Both Capitals are the beginning of period ones.